Direct evidence for minority spin gap in the Co_2MnSi Heusler compound

Stéphane Andrieu,[1,*] Amina Neggache,[1,2] Thomas Hauet,[1] Thibaut Devolder,[3] Ali Hallal,[4] Mairbek Chshiev,[4] Alexandre M. Bataille,[5] Patrick Le Fèvre,[2] and François Bertran[2]

[1]*Institut Jean Lamour, Unité Mixte de Recherche (UMR) 7198, Centre national de la recherche scientifique (CNRS)/Université de Lorraine-BP 239, F-54506 Vandoeuvre Cedex, France*

[2]*Synchrotron SOLEIL, L'Orme des Merisiers, Saint-Aubin, BP 48, 91192 Gif-sur-Yvette Cedex, France*

[3]*Institut d'Electronique Fondamentale, CNRS/Université Paris-Sud/Université Paris Saclay, 91405 Orsay, France*

[4]*Univ. Grenoble Alpes, INAC-SPINTEC, F-38000 Grenoble, France; CNRS, SPINTEC, F-38000 Grenoble, France; and CEA, INAC-SPINTEC, F-38000 Grenoble, France*

[5]*L'Institut rayonnement-matière de Saclay (IRAMIS)/Laboratoire Léon Brillouin (LLB), CEA/Saclay, 91191 Gif-Sur-Yvette, France*

(Received 13 December 2015; published 15 March 2016)

Half metal magnets are of great interest in the field of spintronics because of their potential full spin polarization at the Fermi level (E_F) and low magnetization damping. The high Curie temperature and the predicted 0.7 eV minority spin gap make the Co_2MnSi Heusler compound very promising for applications. We investigated the half-metallic magnetic character of this compound using spin-resolved photoemission, *ab initio* calculation, and ferromagnetic resonance. At the surface of Co_2MnSi, a gap in the minority spin channel is observed, leading to 100% spin polarization. However, this gap is 0.3 eV below E_F, and a minority spin state is observed at E_F. We show that a minority spin gap at E_F can nevertheless be recovered either by changing the chemical composition of the compound or by covering the surface by Mn, MnSi, or MgO. This spin-gap recovery results in extremely small damping coefficients, reaching values as low as 7×10^{-4}.

DOI: 10.1103/PhysRevB.93.094417

I. INTRODUCTION

Although giant magnetoresistance was discovered more than 25 years ago, the development of electronics harnessing the spin of the electron—spintronics—is still very active due to a continuous flow of discoveries [1]. Spintronics devices rely on thin or ultrathin layers of magnetic materials. In most spintronics studies, standard transition metal elements like Fe, Ni, and Co (and alloys thereof) are conveniently used; however, alternative materials with superior electronic properties are desirable. In particular, a class of materials called half metal magnets (HMMs) offers exciting properties both for theory and applications [2]. By definition, HMMs have no minority (or majority) spin states at the Fermi level (E_F): the material is thus a metal for majority (or minority) spins and an insulator for minority (or majority) spins [2–4]. Besides the interest of this full spin polarization for transport properties, extremely low magnetic dampings are also expected. Indeed, because of the minority spin gap, the magnons cannot find the spin-flipping electronic transitions at E_F that systematically degrade the magnon lifetime in standard metallic magnets [5,6]. The expected combined low damping and full spin polarization of HMMs would make them the perfect material for next generation spin transfer torque devices.

Such HMM properties were first observed in magnetic oxides such as Fe_3O_4 [7], CrO_2 [8,9], or $LaSrMnO_3$ (LSMO) [10,11], yet disappointing properties were found, like small magnetizations at remanence or too low Curie temperatures [1]. Other magnetic materials with high T_c, like Heusler compounds, were then explored theoretically [3,4] and produced as thin films in the mid-1990s. The HMM property was claimed for many of them in order to explain transport properties, despite any direct evidence of a spin gap. The shortcoming of this approach was illustrated in the emblematic case of NiMnSb: while a low damping coefficient was measured, consistent with HMM behavior in the bulk material [12], the spin polarization measured using photoemission did not exceed 50% at the surface [13] and felt to zero when covered by MgO [14]. Recently, there was renewed interest after large tunnel magnetoresistance (TMR) was obtained in Co_2MnSi/MgO-based magnetic tunnel junctions (MTJs) [15–17]. The predicted high spin polarization [18,19] was reported very recently (93%) by spin-resolved photoemission spectroscopy (SR-PES) experiments using 21.2 eV photon energy [20]. We show in this paper that this spin polarization at E_F, however, strongly depends on the chosen photon energy in SR-PES measurements. From a device perspective, it is also essential to assess whether this property persists when covering the surface with a thin insulator such as MgO and whether the material has also a low magnetic damping. Here, we thus study the electronic and magnetic properties of Co_2MnSi (noted CMS in the following) by combining SR-PES using various photon energies and ferromagnetic resonance spectroscopy. This motivated the growth of single crystalline CMS films by molecular beam epitaxy (MBE) in order to take advantage of the orbital selectivity of the photoemission process by tuning the linear polarization of the photons. For the bare surface, we observe a total spin gap (100% spin polarization) for the minority spin band but below E_F. At E_F, the spin polarization is reduced by the presence of a minority spin band observed in a very narrow photon energy range that was not explored in Ref. [20]. The possibility to shift this upsetting minority spin band above E_F by stoichiometry engineering [16,21] is examined. We also looked at its suppression by relevant surface hybridization when covered by Mn or MnSi and, more interestingly, by MgO.

*stephane.andrieu@univ-lorraine.fr

II. EXPERIMENTAL AND CALCULATION DETAILS

Calculations are performed using the Vienna *Ab initio* Simulation Package (VASP) [22,23] with generalized gradient approximation [24] and projector- augmented wave pseudopotentials [25,26]. We used the kinetic energy cutoff of 550 eV and a Monkhorst-Pack k-point grid of $11 \times 11 \times 1$ for the surface calculations and $9 \times 9 \times 7$ for the bulk. Initially, the structures were relaxed until the force acting on each atom falls below 1 meV $Å^{-1}$.

The sample preparation and SR-PES measurements were performed at the CASSIOPEE beamline of the SOLEIL synchrotron radiation facility. The CMS samples are grown in a MBE setup connected to the SR-PES chamber [27]. We have worked with MgO (001) substrates, whose lattice constant is close to CMS(001), and which also enable the production of fully epitaxial MgO-based MTJs. We used 2 e-gun sources for Co and Si and a Knudsen cell for Mn. The growth rates were accurately controlled during the growth using quartz microbalances. To get the correct fluxes, a quartz microbalance is located at the place of the sample (prior deposition) that allows us to accurately calibrate the fluxes measured by the other quartz microbalance dedicated to the sources. We estimate the total error on the fluxes less than 5% (even if the quartz measurement is much more accurate, less than 1% with our setup). The film thickness was fixed to 30 nm. The films were heated *in situ* up to 1020 K just after the growth to ensure chemical ordering [28]. The epitaxial process was controlled by using Reflection High Energy Electron Diffraction (RHEED), and the chemical quality of the films was controlled by Auger spectroscopy available in the MBE chamber. The ½ streaks on the RHEED pattern along the [11] azimuth [Fig. 1(a)] are due to the chemical order [29]. The CMS surface is very stable since no contamination was observed by Auger after 24 h PES measurements; neither was there any change on the RHEED patterns [Fig. 1(b)]. It should be noted that, even if Mn and O Auger transitions overlap, the oxygen sensitivity is high on our setup and even a low oxygen contamination can be detected. To illustrate this point, we also show in Fig. 1(b) an Auger spectrum obtained after growing on a CMS film one atomic plane of MgO that contains half a monolayer (ML) of oxygen. It should be noted, however, that the sample heating may lead to surface contamination by O and C (especially for heating temperature above 850 K). Auger spectroscopy was thus systematically performed after the growth and heating of CMS films. Standard x-ray diffraction analysis confirmed the $L2_1$ cubic structure typical of Heusler compounds. The lattice spacing was found to be equal to 0.565 nm in agreement with other published values for CMS. The CMS surface covering was done by Mn, MnSi, or MgO evaporations calibrated using a quartz microbalance. The MgO, Mn, and MnSi grow layer by layer on CMS as checked using RHEED oscillations. This is also an accurate method to determine the growth rates. It should be noted that the ½ streaks shown in Fig. 1(a) are not seen anymore when Mn or MgO are deposited, which is expected according to Mn and MgO (001) surface lattices.

Photoemission was carried out in a spin-resolved photoemission setup using a Mott detector with an overall energy resolution of 150 meV at 37 eV photon energy. The Mott detector

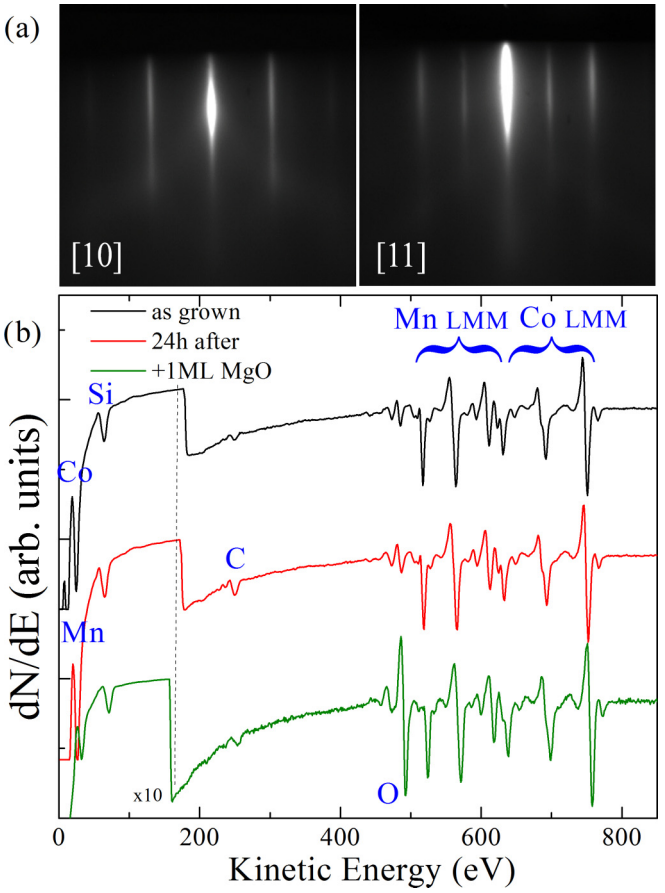

FIG. 1. (a) Typical RHEED patterns observed on the surface of CMS and (b) Auger spectra just after the growth, after 24 hours PES measurements, and for CMS covered by 1 ML of MgO.

is equipped with 4 channels that allowed us to measure spectra for both in-plane and out-of-plane spin components [30]. This Mott detector was operated at a scattering energy equal to 28 keV and with an inelastic energy window equal to 800 eV, leading to a Sherman function equal to 0.12 ± 0.01. This is consistent with the work of Cacho *et al.* [31], where $S = 0.15$ is found at 28 keV using an inelastic energy window of 500 eV. With an inelastic energy window increase from 500 to 800 eV, a 18% decrease of the Sherman function is expected [32], leading to a value equal to 0.123 in agreement with our value. The normal of the sample was oriented along the axis of the detector. The detector angular aperture is fixed at its maximum and is equal to $\pm 8°$, leading to a complete Brillouin zone (BZ) detection along the surface normal with the help of varying photon energy (assuming nonvanishing transition matrix elements for the respective optical transitions). In addition, a certain part of the BZ corresponding to in-plane axes are explored, i.e. around 40% of the BZ along Γ-X at 37 eV photon energy and at normal incidence (be careful that the size of the BZ in a face-centered-cubic (fcc)-like structure along Γ-X is $2\pi/a$ with $a = 0.565$ nm for CMS). To explore the BZ along Γ-X, we also rotated the sample off-normal by 8° from the detector axis. Similar transitions are observed for both measurement angles, meaning that the whole BZ is explored. To eliminate instrumental asymmetry in spin-resolved measurements, two distinct PES spectra were

recorded with opposite magnetizations. As the coercive field of our CMS films was less than 20 Oe, the applied magnetic field was set to 200 Oe to saturate the magnetization prior to PES measurements. We systematically observed a zero out-of-plane spin polarization, confirming that the magnetization of our CMS films was in plane. The symmetry of the initial states involved in the transitions observed on SR-PES spectra was determined by measuring successively with s or p polarizations of the incoming photons. As the photon beam was at 45° from the normal to the sample, s-polarized photons excite only occupied $\Delta 5$ states, whereas p-polarized photons excite both occupied $\Delta 1$ and $\Delta 5$ states [33,34]. The SR-PES analysis was performed using incoming photon energy ranging from 20 to 110 eV. The PES measurements were performed both at 300 or 80 K. We do not observe any significant influence of the sample temperature on the PES results. Around 40 samples were grown and measured during 6 runs of 1 week each.

The dynamic magnetic properties of Au-covered CMS samples were determined by using vector network analyzer ferromagnetic resonance (VNAFMR) [35] in both in-plane and out-of-plane applied fields. The FMR frequency-field relation provides the effective magnetization. An estimate of the Gilbert damping can be done by fitting the evolution of the linewidth with the resonance frequency in perpendicular applied field.

III. RESULTS

We first looked at the spin polarization of the uncoated surface, both theoretically and experimentally. In order to test the HMM character of Co_2MnSi, we first performed *ab initio* calculations considering the Heusler structure without surfaces [bulk, Fig. 2(a)] or with different surface terminations [Figs. 2(b)–2(d)]. As shown in Fig. 2(a), a spin gap of about 0.7 eV is predicted in the calculated density of states (DOS) for bulk CMS (with no surface included in the calculation). This gap is, however, strongly affected, taking into account the surface: it is destroyed by terminating the crystal with Co, recovered when terminating with Mn, but also with MgO. These results are in agreement with previous calculations performed on CMS varying the surface termination [36] and on CMS/MgO/CMS magnetic tunnel junctions [37]. We examined these different cases in practice, and we focused first on as-grown CMS layers. Majority and minority SR-PES spectra at room temperature for the bare CMS are shown in Fig. 3(a). The 100% spin polarization is confirmed experimentally since the minority spin spectrum reaches zero for a binding energy around −0.3 eV. It should be noted that heating up to 1020 K is necessary to get the correct chemical ordering and the 100% spin polarization in agreement with Ref. [28] (heating up to 870 K only leads to 80% on our samples). The spin gap is thus observed below E_F, while *ab initio* calculations performed considering bulk CMS predicted it to span upon E_F. It does not extend up to E_F because of a minority spin contribution at E_F [transition noted A in Fig. 3(b)]. It should be noted that this contribution is not observed in DOS calculations in Fig. 2. Additionally, there is also a majority spin contribution around −0.4 eV [transition B in Fig. 3(b)] which also does not appear in the bulk calculations. To shed light on the origin of these A and B transitions, we have rotated the photon polarization in order to determine the symmetry of the states involved. The

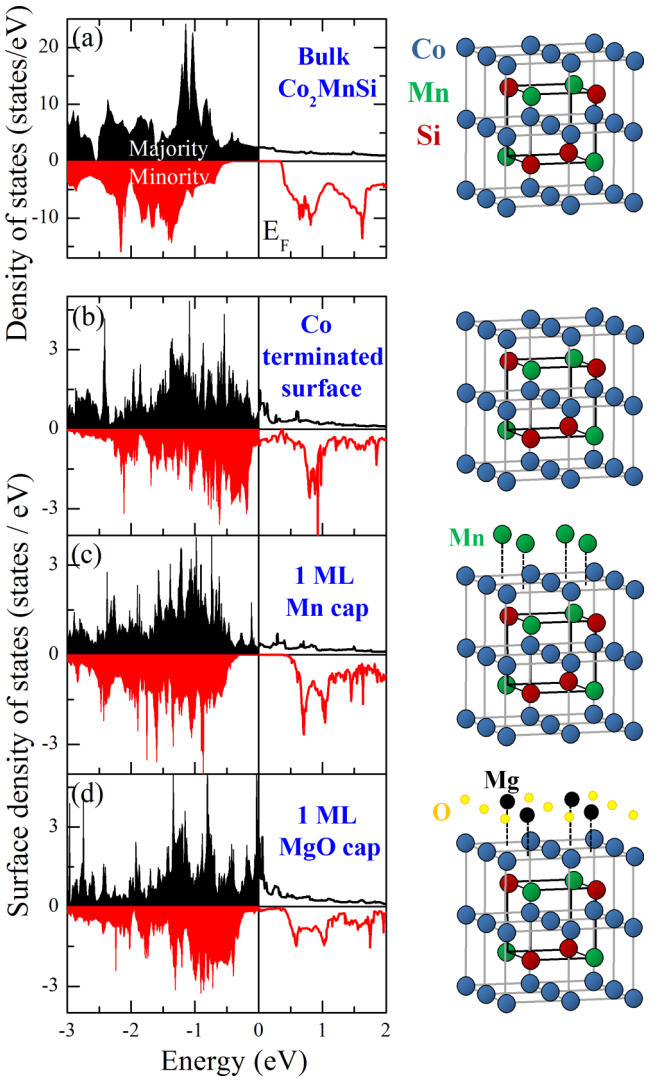

FIG. 2. (a) Full DOS for both spins calculated for the bulk (with no surface) and surface contribution to the DOS for (b) a Co-terminated surface, (c) 1 Mn atomic plane on top, and (d) 1 MgO atomic plane on top. The structures are shown on the right.

PES spectra obtained for p and s polarizations are compared in Figs. 3(b) and 3(c). The p polarization excites electronic states with $\Delta 1$ and $\Delta 5$ symmetries, while the s polarization only excites $\Delta 5$ states. The loss of intensity, for the A and B transitions, when going from p to s polarization demonstrates that they are both of $\Delta 1$ character. Interestingly, when the use of s polarization suppresses the A and B transitions, the PES recovers consistency with the DOS calculated in the bulk: the spin gap now straddles E_F down to −0.4 eV, in very good agreement with calculations (Fig. 2). This is a strong indication that A and B contributions are linked to the surface. A majority spin surface resonant state was indeed predicted by Braun *et al.* [38] using *ab initio* calculations that can account for the B transition. However, it is calculated at 0.4 eV above E_F, whereas the B transition is here observed below E_F. It seems to be also observed in a recent work using 6 eV photon energy, with the same polarization dependence [39]. On the contrary, the A contribution was not observed in Ref. [20]. This was due to the used photon energy (21.2 eV). Indeed, we

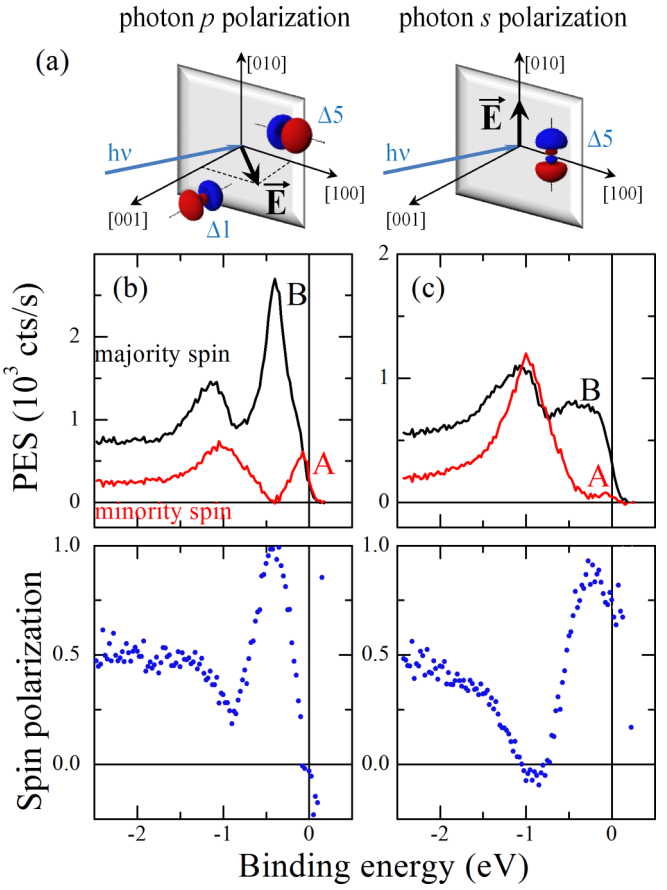

FIG. 3. Dependence of PES results on a Co_2MnSi film upon light polarization and excited photon energy. (a) Schematic of the excited states depending on the light polarization. Spin-resolved and PES spectra using the (b) *p* and (c) *s* polarizations of the 37 eV incoming photons performed on the same CMS sample. The two peaks named A and B observed using the *p* polarization are strongly attenuated using *s* polarization, meaning that the initial state symmetry is Δ1. The spin gap is thus observed to extend up to E_F. The energy resolution is 150 meV.

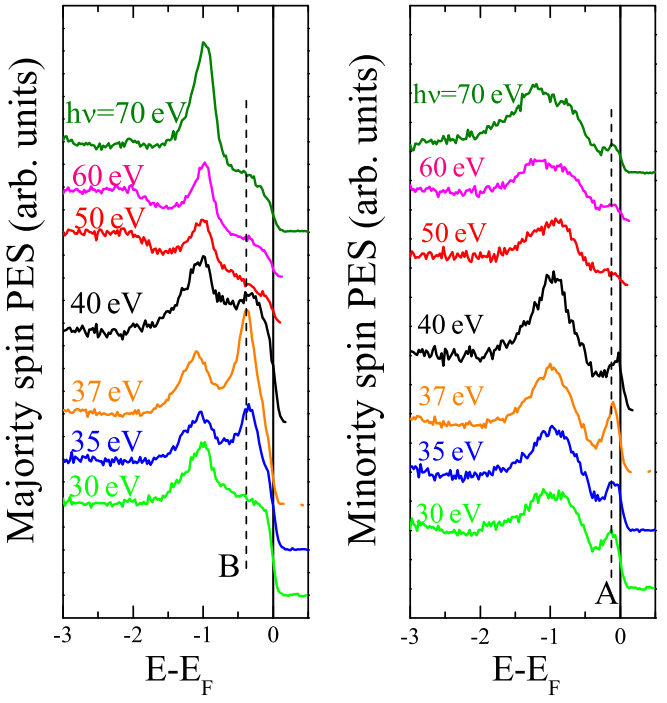

FIG. 4. PES spectra dependence with the photon energy using *p* polarization, for both majority and minority spins, on a Co_2MnSi layer. The A and B peaks are strongly affected by any change of the exciting photon energy, showing a resonant behavior between 35 and 40 eV.

observed that these A and B transitions are only detected in a very narrow photon energy range from around 35 to 40 eV (Fig. 4). Any measurement out of this photon energy range thus misleadingly leads to strong positive spin polarization at E_F. The PES off-normal experiment (at 4° and 8° from the normal of the surface) also shows that the A and B contributions decreased compared to measurement at normal incidence, meaning that these states are located around Γ. Finally, since those states are likely to be detrimental to magnetotransport properties, let us design strategies to mitigate their impact.

One solution should be to decrease E_F by decreasing the number of valence band electrons in order to push the A contribution in empty states. This goal can be reached by changing the compound stoichiometry as shown in Fig. 5. Indeed, Ishikawa *et al.* [16] studied magnetotransport in CMS/MgO/CMS MTJs and found a surprising result: the maximum of tunnel magnetoresistance was not observed for the exact CMS stoichiometry, but for an excess of Mn. To understand this behavior, we performed a SR-PES analysis on several samples with different Mn contents like in their study. We have studied both a simple excess of Mn and a partial replacement of Co by Mn, with qualitatively similar conclusions. Photoemission spectroscopy spectra obtained for 1, 1.1, and 1.2 relative concentration of Mn in Co_2Mn_xSi are plotted in Fig. 5. As Ishikawa *et al.* [16] did, we heated the CMS layers only up to 870 K. At this temperature, the chemical ordering in the unit cell is incomplete, and correlatively, the spin polarization reaches 80% instead of the 100% that can be obtained after annealing above 1000 K. Increasing the Mn content shifts the maximum of the spin polarization peak towards E_F, which explains the conclusions drawn from magnetotransport. In fact, this shift of the spin gap can be understood from hand waving arguments. Indeed, replacing Co by Mn reduces the number of valence electrons available to fill the DOS. In a rigid band structure picture, this electron depletion moves E_F closer to the spin gap as the Mn content is increased (Fig. 5). This also means that the minority spin contribution A is pushed towards empty states leading to high spin polarization at E_F when enriching with Mn. Our experiments thus clearly explain the tunnel magnetoresistance increase when increasing the Mn content reported in Ref. [16].

The next step in our study was to look at the influence of the CMS layer capping on the spin polarization. As we have seen in Fig. 2, the A and B contributions are not reproduced by calculations of the bulk DOS. One may assume that the A and B states result from chemical disorder in the bulk [40]. In this case, capping the CMS would not change that situation, in stark contradiction with our results. A more plausible explanation is that the A and B transitions involve surface states. To test this, we first looked at the dispersion of these states along the (001)

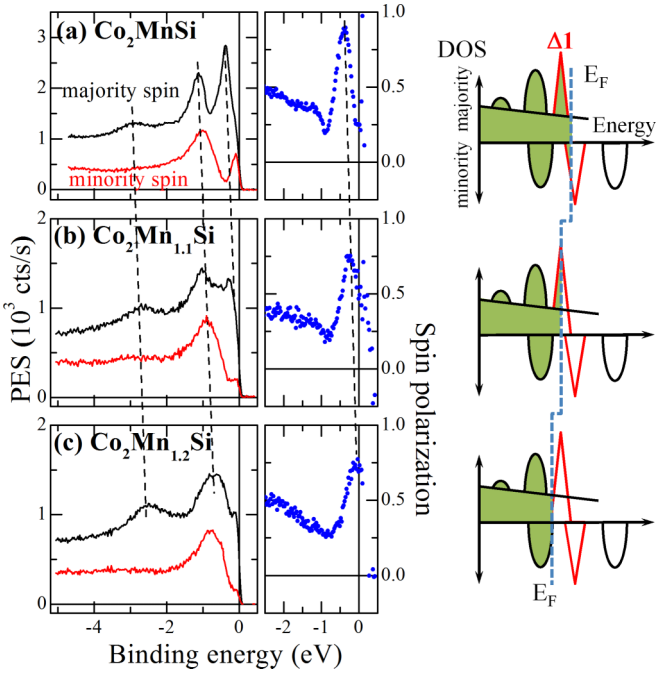

FIG. 5. SR-PES spectra at 300 K using p polarization and $h\nu = 37$ eV for a series of CMS layers with increasing Mn content. As shown in the schemes, E_F is moving towards the spin polarization maximum when increasing the Mn content.

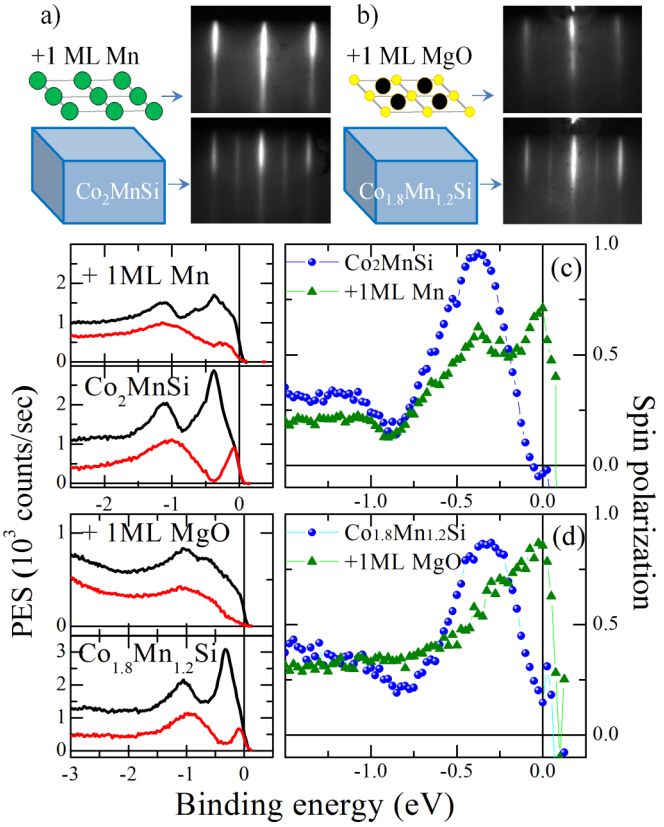

FIG. 6. Influence of Mn and MgO coverage on CMS electronic properties. In (a) and (b) are shown the electron diffraction patterns for the starting CMS layers and when covered by Mn or MgO. The PES and spin-polarization spectra for the starting CMS layers and after the capping are shown in (c) Mn cap and (d) MgO cap. As the spin polarization is close to zero at E_F for both CMS uncoated surfaces, it is strongly increased when covering with Mn or MgO.

direction by varying the photon energy from 20 to 110 eV to scan the wave vector component perpendicular to the surface, the lack of dispersion of this component being a necessary condition for a surface state. Unfortunately, these transitions were only observed in the range of photon energy from 35 to 40 eV, i.e. too narrow to assess the state dispersion (Fig. 4). Such a resonant photoemission process was already observed on surface states [41,42]. However, the photon energy range involved here is very small compared to observations done on noble metal surfaces for instance. One way to understand this behavior is looking at the origin of these states. Usually, surface states are created because of the broken symmetry of the crystal due to the surface. In our case, another scenario may be proposed considering that the surface chemistry is not similar to the bulk one. Even if a strict comparison between band structure calculation and PES experiments is often delicate (see for instance Ref. [27]), it is quite surprising that these A and B states are absent from the band structure calculation. This is a strong indication that the chemistry of the surface termination is at the origin of these states.

To conclude on the physical mechanism determining the surface spin polarization, we decided to cap the CMS with various overlayers. Galanakis [43] indeed showed by *ab initio* calculations performed on Co_2MnGe that the spin gap may be strongly affected by the surface termination. To verify whether this applies in our case, we calculated the DOS with different types of overlayers (Fig. 2). Whereas the spin gap is not obtained at E_F with a bare CMS surface, in good agreement with Ref. [44], it is predicted to be retrieved when terminated with a Mn ML. We thus deposited one Mn ML on top of a CMS layer. We observed that the A and B contributions are strongly decreased, while the spin polarization strongly increased at E_F [Figs. 6(a) and 6(c)]. We also tested MnSi termination and observed the same effect, but more interestingly, as predicted by calculation [Fig. 2(d)], a thin MgO termination is also efficient to retrieve the minority spin gap. Indeed, the measured spin polarization at E_F increases up to around +70% (from 60 to 80% from one sample to the other) by adding MgO. This is larger than in previous works using also SR-PES, but with very low photon energy [39,45]. Moreover, an even larger spin polarization at E_F (90%) was obtained by using a Mn-enriched $Co_{1.8}Mn_{1.2}Si$ layer covered by MgO [Figs. 6(b) and 6(d)]. The possibility to tune the spin polarization at E_F, both with CMS stoichiometry and MgO covering, is a very promising result and contrasts with the NiMnSb/MgO system [14]. Altogether, these experiments are a strong indication that A and B contributions are probably from similar bands originating from the surface and separated in energy by exchange splitting of the electronic states due to the ferromagnetic behavior. Although the agreement between the calculated DOS and measured PES is not quantitative, the observed enhancement of spin polarization at E_F due to MgO and Mn coverage (as compared to free CMS) is qualitatively explained.

To fulfill the demonstration of the HMM behavior of bulk CMS, we performed Gilbert damping measurements on the samples studied by SR-PES (bare surface and Mn-, MnSi-,

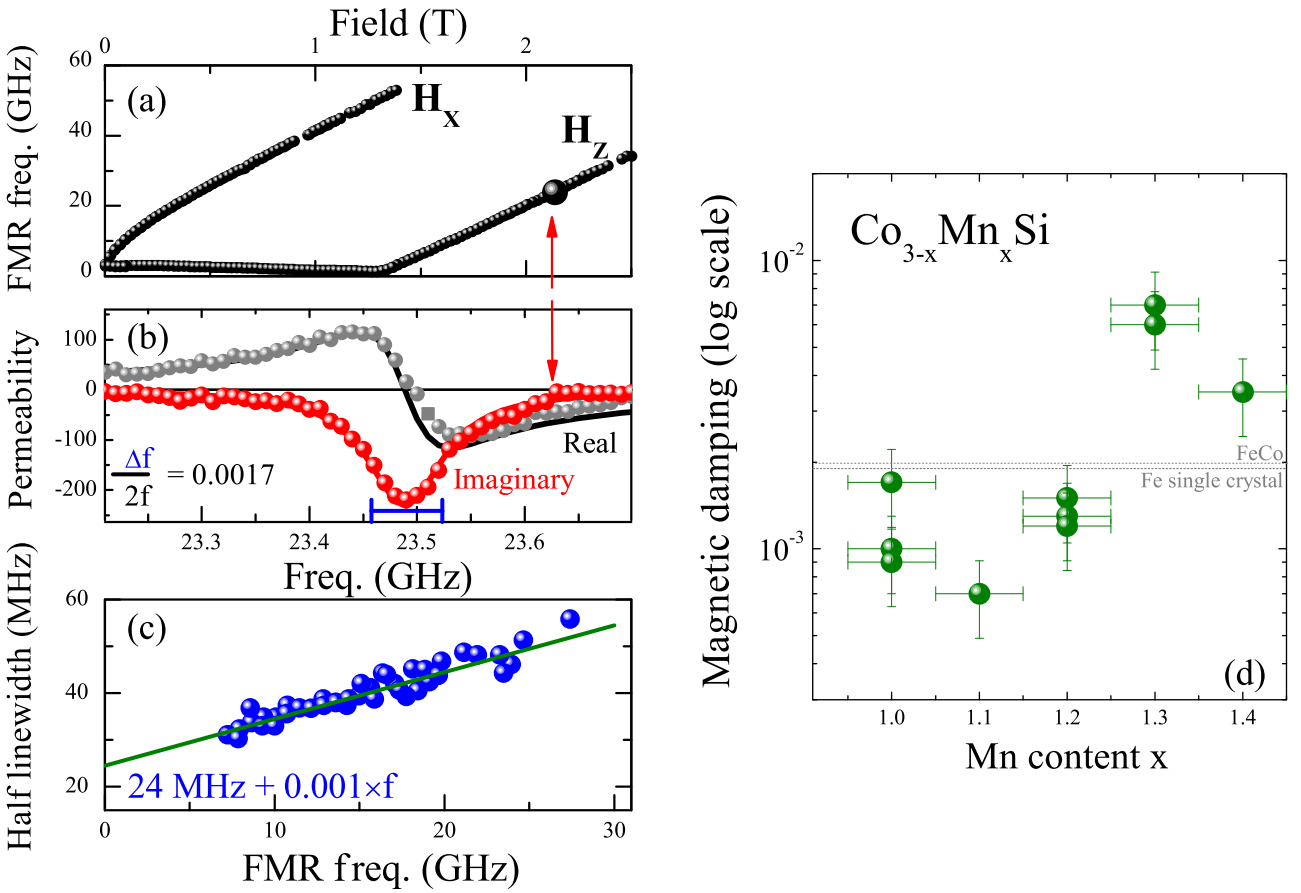

FIG. 7. FMR properties of 30 nm thick CMS film. (a) Frequency versus field plots for in-plane (H_x) and out-of-plane (H_z) applied fields. (b) Real and imaginary parts of the experimental (symbols) and modeled (lines) permeability for an out-of-plane field of 2.1 T. (c) Frequency linewidth versus FMR frequency in H_z field. The line is a linear fit. In (d) is plotted the magnetic damping coefficients obtained by FMR on a series of $Co_{3-x}Mn_xSi$ samples. The damping obtained in single crystalline Fe thin films [47] and FeCo equimolar alloy [48] are indicated on the graph (d) for comparison.

or MgO-capped surfaces) that were capped with 5 nm Au before moving them out from ultrahigh vacuum (UHV). Gilbert damping can be viewed as a measure of the decay rate of the population of low energy magnons. In magnetic metals, magnons decay mostly when they are annihilated by collisions with electrons whose spin is flipped in that process [46]. Since the energy of the magnons that matter for magnetization dynamics lies in the 10 μeV range, the transitions involve only electronic states very close to E_F. These transitions do not exist in HMM, such that their damping should be comparable to that of insulators. We thus measured the dynamic magnetic properties of Au-covered CMS samples using VNAFMR [35] in both in-plane and out-of-plane applied fields (Fig. 7). The effective magnetization appeared to depend strongly on the temperature at which the CMS was postgrowth annealed. The largest magnetizations (1.25 T) were obtained for samples heated at 1020 K, where chemical order was the most complete. On these samples, the FMR lines were particularly narrow, with raw linewidths already smaller than the best ever measured using the same setup on iron [47]. We found Gilbert damping values close to 10^{-3} on a series of $Co_{3-x}Mn_xSi$ samples, and a record value of 7.10^{-4} observed on a $Co_{1.9}Mn_{1.1}Si$ sample. Such values are extremely low for a conductive material (and to our knowledge lowest than the best one reported in Fe ($1.9\,10^{-3}$) [47], FeCo (2.10^{-3}) [48], or some Co-based Heusler compounds ($>5.10^{-3}$) [49]), and are consistent with a HMM behavior at least in the bulk of CMS.

IV. CONCLUSIONS

In summary, we experimentally established that the CMS Heusler compound is a HMM in its bulk, but altered at the surface by the presence of surface states of $\Delta 1$ character, close to E_F in both minority and majority spin channels. Enriching the CMS compound with Mn lowers its E_F below the surface states. This clarifies the dependence of tunnel magnetoresistance on the compound stoichiometry. Moreover, we also proved that these states are strongly linked to the surface termination of CMS and that they can be almost suppressed when covering CMS with Mn, MnSi, and MgO. The HMM character comes with extremely low values of Gilbert damping, which reaches values never observed before on conducting materials. All of these results make the CMS/MgO system an excellent candidate for the study of spin-related phenomena and the related applications in spintronics.

ACKNOWLEDGMENTS

We would like to thank A.D. Kent from New York University for his critical reading of the paper, F. Solal from Rennes University (France), and D. Malterre from Institut Jean Lamour/Lorraine University (France) for fruitful discussion on the PES results. This work was supported by the Region Lorraine. The theoretical work using ab initio calculations was partly supported by the M-ERA.NET Project HEUMEM ANR-14-MERA-0001-02.

[1] See for instance A. Fert, J. M. George, H. Jaffrès, R. Mattana, and P. Seneor, Europhys. News **34**, 227 (2003).
[2] R. A. de Groot, F. M. Mueller, P. G. van Engen, and K. H. J. Buschow, Phys. Rev. Lett. **50**, 2024 (1983).
[3] See for instance I. Galanakis and P. Mavropoulos, J. Phys. Condens. Matter **19**, 315213 (2007).
[4] For a review see T. Graf, C. Felser, and S. S. P. Parkin, Prog. Solid State Ch. **39**, 1 (2011).
[5] P. Buczek, A. Ernst, P. Bruno, and L. M. Sandratskii, Phys. Rev. Lett. **102**, 247206 (2009).
[6] C. Liu, C. K. A. Mewes, M. Chshiev, T. Mewes, and W. H. Butler, Appl. Phys. Lett. **95**, 022509 (2009).
[7] M. I. Katsnelson, V. Y. Irkhin, L. Chioncel, A. I. Lichtenstein, and R. Z. de Groot, Rev. Mod. Phys. **80**, 315 (2008).
[8] K. Schwarz, J. Phys. F: Met. Phys. **16**, L211 (1986).
[9] K. P. Kämper, W. Schmitt, G. Guntherodt, R. J. Gambino, and R. Ruf, Phys. Rev. Lett. **59**, 2788 (1987).
[10] W. E. Pickett and D. J. Singh, J. Magn. Magn. Mater. **172**, 237 (1997).
[11] J. H. Park, E. Vescovo, H-J. Kim, C. Kwon, R. Ramesh, and T. Venkatesan, Nature (London) **392**, 794 (1998).
[12] B. Pigeau, G. de Loubens, O. Klein, A. Riegler, F. Lochner, G. Schmidt, L. W. Molenkamp, V. S. Tiberkevich, and A. N. Slavin, Appl. Phys. Lett. **96**, 132506 (2010).
[13] G. L. Bona, F. Meier, M. Taborelli, E. Bucher,and P. H. Schmidt, Solid State Commun. **56**, 391 (1985).
[14] M. Sicot, P. Turban, S. Andrieu, A. Tagliaferri, C. de Nadai, N. B. Brookes, F. Bertran, and F. Fortuna, J. Magn. Magn. Mater. **303**, 54 (2006).
[15] Y. Sakuraba, M. Hattori, M. Oogane, Y. Ando, H. Kato, A. Sakuma, T. Miyazaki, and H. Kubota, Appl. Phys. Lett. **88**, 192508 (2006).
[16] T. Ishikawa, H-X Liu, T. Taira, K-I Matsuda, T. Uemura, and M. Yamamoto, Appl. Phys. Lett. **95**, 232512 (2009).
[17] H.-X. Liu, Y. Honda, T. Taira, K-I. Matsuda, M. Arita, T. Uemura, and M. Yamamoto, Appl. Phys. Lett. **101**, 132418 (2012).
[18] S. Ishida, S. Fujii, S. Kashiwagi, and S. Asano, J. Phys. Soc. Japan **64**, 2152 (1995).
[19] S. Picozzi, A. Continenza, and A. J. Freeman, Phys. Rev. B **66**, 094421 (2002).
[20] M. Jourdan, J. Minar, J. Braun, A. Kronenberg, S. Chadov, B. Balke, A. Gloskovskii, M. Kolbe, H. J. Elmers, G. Schonhense, H. Ebert, C. Felser, and M. Klaui, Nat. Commun. **5**, 3974 (2014).
[21] J. P. Wustenberg, R. Fetzer, M. Aeschlimann, M. Cinchetti, J. Minar, J. Braun, H. Ebert, T. Ishikawa, T. Uemura, and M. Yamamoto. Phys. Rev. B **85**, 064407 (2012).
[22] G. Kresse and J. Hafner, Phys. Rev. B **47**, 558(R) (1993).
[23] G. Kresse and J. Furthmüller, Phys. Rev. B **54**, 11169 (1996).
[24] Y. Wang and J. P. Perdew, Phys. Rev. B **44**, 13298 (1991).
[25] G. Kresse and D. Joubert, Phys. Rev. B **59**, 1758 (1999).
[26] P. E. Blöchl, Phys. Rev. B **50**, 17953 (1994).
[27] S. Andrieu, L. Calmels, T. Hauet, F. Bonell, P. Le Fèvre, and F. Bertran, Phys. Rev. B **90**, 214406 (2014).
[28] G. Ortiz, A. Garcia-Garcia, N. Biziere, F. Boust, J. F Bobo, and E. Snoeck, J. Appl. Phys. **113**, 043921 (2013).
[29] A. Neggache, T. Hauet, F. Bertran, P. Le Fèvre, S. Petit-Watelot, T. Devolder, Ph. Ohresser, P. Boulet, C. Mewes, S. Maat, J. R. Childress, and S. Andrieu, Appl. Phys. Lett. **104**, 252412 (2014).
[30] F. Ciccacci, S. De Rossi, and D. M. Campbell, Rev. Sci. Instrum. **66**, 4161 (1995).
[31] C. M. Cacho, S. Vlaic, M. Malvestuto, B. Ressel, E. A. Seddon, and F. Parmigiani, Rev. Sci. Instrum. **80**, 043904 (2009).
[32] S. Qiao, A. Kimura, A. Harasawa, M. Sawada, J.-G. Chung, and A. Kakizaki, Rev. Sci. Instrum. **68**, 4390 (1997).
[33] P. D. Johnson, Rep. Prog. Phys. **60**, 1217 (1997).
[34] F. Bonell, T. Hauet, S. Andrieu, F. Bertran, P. Le Fèvre, L. Calmels, A. Tejeda, F. Montaigne, B. Warot-Fonrose, B. Belhadji, A. Nicolaou, and A. Taleb-Ibrahimi, Phys. Rev. Lett. **108**, 176602 (2012).
[35] C. Bilzer, T. Devolder, P. Crozat, and C. Chappert, IEEE Trans. Magn. **44**, 3265 (2008).
[36] S. J. Hashemifar, P. Kratzer, and M. Scheffler, Phys. Rev. Lett. **94**, 096402 (2005).
[37] Y. Miura, H. Uchida, Y. Oba, K. Abe, and M. Shirai, Phys. Rev. B **78**, 064416 (2008).
[38] J. Braun, M. Jourdan, A. Kronenberg, S. Chadov, B. Balke, M. Kolbe, A. Gloskovskii, H. J. Elmers, G. Schonhense, C. Felser, M. Klaui, H. Ebert, and J. Minar, Phys. Rev B **91**, 195128 (2015).
[39] R. Fetzer, B. Stadtmuller, Y. Ohdaira, H. Naganuma, M. Oogane, Y. Ando, T. Taira, T. Uemura, M. Yamamoto, M. Aeschlimann, and M. Cinchetti, Sci. Rep. **5**, 8537 (2015).
[40] S. Picozzi, A. Continenza, and A. J. Freeman, Phys. Rev. B **69**, 094423 (2004).
[41] S. G. Louie, P. Thiry, R. Pinchaux, Y. Petroff, D. Chandesris, and J. Lecante, Phys. Rev. Lett. **44**, 549 (1980).
[42] S. D. Kevan and R. H. Gaylord, Phys. Rev. B **36**, 5809 (1987).
[43] I. Galanakis, J. Phys. Condens. Matter **14**, 6329 (2002).
[44] Y. Miura, K. Abe, and M. Shirai, Phys. Rev. B **83**, 214411 (2011).
[45] R. Fetzer, J. P. Wustenberg, T. Taira, T. Uemura, M. Yamamoto, M. Aeschlimann, and M. Cinchetti, Phys. Rev. B **87**, 184418 (2013).
[46] V. Kamberský, Czech. J. Phys. B **26**, 1366 (1976).
[47] T. Devolder, M. Manfrini, T. Hauet and S. Andrieu, Appl. Phys. Lett. **103**, 242410 (2013).
[48] M. Oogane, T. Wakitani, S. Yakata, R. Yilgin, Y. Ando, A. Sakuma, and T. Miyazaki, Jpn. J. Appl. Phys. **45**, 3889 (2006).
[49] M. Oogane, T. Kubota, H. Naganuma, and Y. Ando, J. Phys. D: Appl. Phys. **48**, 164012 (2015).